Noise Correlation in Silicon Spin Qubits: A Computational Study

Guoting Cheng

Department of Electrical & Computer Engineering

University of Florida

Gainesville, FL, USA

guoting.cheng@ufl.edu

Jing Guo
Department of Electrical & Computer Engineering
University of Florida
Gainesville, FL, USA
guoj@ufl.edu

Abstract—The platform of silicon-based spin qubits holds significant potential for the hardware implementation of quantum computing. Charge noise, however, notably hinders the performance and scalability of silicon-spin-based quantum computing technologies. Here we computationally investigated correlated charge noise in silicon spin quantum computing devices by developing and applying a Green's transfer function approach. The approach allows for the systematic simulation and analysis of both the noise's auto-correlation and cross-correlation spectrums in a physics-based manner. We simulate the correlated noise's power spectral density (PSD) in silicon spin qubit devices. The results indicate strong cross-correlation and show phase-flipping features in neighboring silicon spin qubits, in agreement with a recent experiment. Given that each spin qubit device is small and influenced by a limited number of two-level fluctuators (TLFs), the arrangement of these TLFs plays a crucial role in the correlation of noise. The simulation study highlights the need to consider noise correlation and its related spectral features in developing robust quantum computing technologies based on silicon spin qubits.

Index Terms—qubit, silicon, quantum computing device, quantum noise, correlation

I. Introduction

Noise presents a significant barrier in advancing quantum computing technologies [1]. In semiconductor-spin-based quantum computing [2]-[4], various noise sources, such as charge noise and nuclear magnetic noise, impact the system's performance [5], [6]. Despite notable advances in reducing noise and enhancing the fidelity of quantum gates [7]–[10], noise remains a primary challenge in achieving higher fidelity and scalability in silicon-based quantum systems. Charge noise in semiconductor spin qubits typically exhibits a 1/f-like power spectrum, often linked to two-level fluctuators (TLFs) [5], [11]–[13]. With the miniaturization of semiconductor spin qubit devices and higher integration densities, noise correlations across adjacent qubits and quantum gates become more pronounced. Recent studies have focused on examining noise correlation patterns in silicon spin qubits, revealing phaseflipping phenomena in the noise correlation spectrum among neighboring qubits [14]. This highlights the importance and need of developing physical models and understanding noise correlations to devise effective noise mitigation strategies,

This work was supported by NSF Grants #2007200 and #2142552.

which are crucial for improved fidelity and scalability of quantum computing systems utilizing silicon spin qubits.

This study introduces a method based on Green's transfer function to model the noise correlation spectra in siliconbased spin qubits. This method links the behavior of TLFs, which are the charge noise sources, with the observed noise spectra in spin qubit devices via a Green's transfer function. The method provides a systematic way to simulate both the auto-correlation and cross-correlation of noise spectra in these devices. Through this simulation technique, we investigate the correlated noise in terms of power spectral density (PSD) between the precession frequencies and exchange interactions in neighboring silicon spin qubits. Given the nanoscale dimensions of silicon spin qubit devices, a small number of discrete TLFs play a determinant role in their noise characteristics. Our findings indicate a significant presence of noise crosscorrelation within these devices, emphasizing the impact of random, discrete TLFs on the noise spectrum. Furthermore, the study offers insights into the experimentally observed phase flipping in the cross-PSD between neighboring qubits [14]. This work advances modeling methods and understanding of noise correlation in silicon spin qubit devices, which is an important step toward developing robust and scalable quantum computing systems based on silicon electron spins.

II. APPROACH

Figure 1 shows the modeled device structure of a two-qubit quantum gate between neighboring spin qubits [14]. Experimentally, both a SiGe-Si heterostructure and silicon metal-oxide-semiconductor (MOS) structure have been used to fabricate silicon spin qubits [15]. In a SiGe-Si heterostructure, a thin silicon layer is sandwiched between SiGe layers. In a MOS structure, electrons are confined vertically by a potential well at the SiO₂-Si interface. The two quantum dots can be defined by applying gate voltages to the plunger gates (PGs), which operate the qubit pairs at the (1,1) electron number regime. The tunnel barriers between the QDs can be modulated by the barrier gate (BG). A thin oxide layer separates the gates with the top SiGe layer in the SiGe-Si heterostructure.

Green's transfer function method: We extend the Green's transfer function method, which has been used in noise analysis of metal-oxide-semiconductor (MOS) FETs [16], to

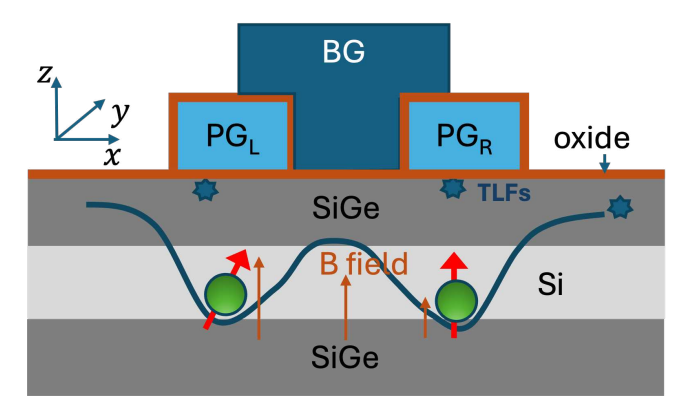


Fig. 1: Schematic structure of the modeled spin qubit device in silicon. The QDs are defined by the left and right plunger gates, PG_L and PG_R . The tunnel barrier can be modulated by the barrier gate (BG). A silicon layer is confined between SiGe in a SiGe-Si heterostructure. The non-uniform magnetic field, B field is denoted. The randomly distributed TLFs are shown schematically as stars.

noise analysis of semiconductor qubit devices. Charge fluctuation in TLFs creates a stochastic electric field perturbation to qubits and their exchange interactions. TLFs have been generally identified as the source of charge noise [13], although their microscopic physical origins remain an open question. For noise in a spin qubit system of N qubits, we define a vector of the physical quantities of interest $P = [\nu_1, ...\nu_m, ..., \nu_N, ..., J_{mn}, ...]$, where ν_m is the precession frequency of each qubit, J_{mn} is the exchange interaction (in a unit of Hertz) between a pair of qubit (m, n). The autocorrelation function between the i_{th} and j_{th} elements of P, $R_{ij}(t) = \langle P_i(0)P_j(t)\rangle$ forms a matrix. Its Fourier transform is the PSD matrix $S(f) = \mathcal{F}(R(t))$, which can be computed from the PSD of the noise source K(f),

$$S(f) = G(f)K(f)G(f)^{+}, \tag{1}$$

where G(f) is the Green's transfer function matrix. At the low-frequency noise region, G(f) can be treated quasi-statically and is frequency-independent. The diagonal element of S(f) gives the noise PSD of the physical quantities of interest. The off-diagonal elements compute the noise correlation between the ith and jth physical quantity of interest,

$$C_{ij}(f) = S_{ij}(f) / \sqrt{S_{ii}(f)S_{jj}(f)}.$$
 (2)

Model TLFs: TLFs have been widely considered an important noise source in various quantum computing hardware platforms [13], [17]–[19]. In superconductor qubits, TLFs are known to be approximately uniformly distributed across a wide range of frequencies. They possess both elastic and electric dipole moments, enabling them to interact with both mechanical deformation and electrical fields [17], [18]. In semiconductor qubits, the dynamics of TLFs have been characterized and modeled [13], [19]. Nonetheless, what these TLFs microscopically are and where exactly they are located are still open questions. In a simplified model, charge noise

in semiconductors can be due to TLF defects capable of capturing and emitting charges [20], [21]. The TLFs do not exchange charge with the QDs but can exchange charge with their environment, inducing carrier reservoirs of electrodes, and nearby two-dimensional electron gas [13]. TLFs are not only limited to a whole electron charge fluctuation, in which a carrier is trapped and emitted but also include dipolar fluctuations where a charge fluctuates between two positions within a double-well setup [22], [23]. The TLFs are assumed to follow the dynamics of random telegraph noise (RTN) with a characteristic transition time of τ_{Tk} [11], [20]. The Fourier transform of its autocorrelation function of the TLF charge gives its power spectral density (PSD) in the form of a Lorentzian function with a corner frequency of $f_{Tk} = 1/(2\pi\tau_{Tk})$ The matrix elements of the noise source of the correlation has a Debue-Lorentzian spectrum [24],

$$K_{kl}\left(f\right) = \frac{1}{2} \frac{\tau_{Tk}}{1 + \left(2\pi f \tau_{Tk}\right)^2} \delta_{kl} \tag{3}$$

where δ_{kl} is the Kronecker delta, and τ_{Tk} is the transition time of the kth TLF. As shown in Fig. 1, the experimental characterization and modeling of the transition rate of TLFs have been conducted [13]. However, the microscopic origins of TLFs remain an open question, leading to a lack of detailed physical understanding regarding their transition time. It is assumed that TLFs do not exchange charge with the QDs. Consequently, the transition time appears to be primarily influenced by the interactions among TLFs themselves and their surrounding environment, rather than by interactions with the QDs [23]. The transition rates of TLFs have shown ranges of distributions and dependence on gate voltages and temperatures, which are still not fully understood [13], [22], Here, we use a random log-uniform distribution of the transition time of TLFs in a given transition time range [23].

Model Green's transfer function: TLFs result in a Coulombic field. A silicon spin qubit device has a nanoscale dimension. Only a small number of TLFs are involved for each device. For the kth TLF located at an in-plane position of (X_{Tk}, Y_{Tk}) , and a depth of d_{Tk} from the interface, by using the Thomas-Fermi (TF) approximation, the screened potential can be expressed as [25], [26],

$$U_{Tk}(r) = \frac{1}{(2\pi)^2} \int_0^\infty q dq \int_0^{2\pi} d\theta \, V_{scr}(q) \, e^{iqr\cos(\theta)} \tag{4}$$

where

$$V_{scr}(q) = \frac{e^2}{2\varepsilon_{si}} \frac{e^{-qd}}{q + q_{TF}},\tag{5}$$

 $r(x,y) = \sqrt{\left(x - X_{Tk}\right)^2 + \left(y - Y_{Tk}\right)^2}, \ e \ \text{is the elementary electron charge, } \varepsilon_{si} \ \text{is the silicon dielectric constant, } q_{TF} \approx 2/(3nm) \ \text{is the TF screening wave vector [26]. The in-plane electrostatic force is computed as } \vec{F}_{Tk}(x,y) = -\nabla U_{Tk}(x,y).$ The potential at the *i*th QD dot can be evaluated as $U_{ik} = \langle \psi_i(x,y) | U_{TK}(x,y) | \psi_i(x,y) \rangle$, and the force is computed as $\vec{F}_{ik} = \langle \psi_i(x,y) | \vec{F}_{Tk}(x,y) | \psi_i(x,y) \rangle$. where $\psi_i(x,y)$ is the

confined electron wave function. The wavefunction takes a Gaussian form [27] with a quadratic QD confinement potential $V_{conf}(x,y)=\frac{1}{2}m^*\omega^2((x-x_c)^2+(y-y_c)^2)$, where the QD center is at (x_c,y_c) , $m^*=0.19m_0$ is the in-plane effective mass of the silicon layer and m_0 is the free electron mass, and a value of $\hbar\omega=5meV$ is used in this study, which results in a Gaussian form of the wave function with a characteristic radial length of $l_{QD}=\sqrt{\hbar/(m^*\omega)})\approx 9.0nm$. The values are nominal and typical for a semiconductor QD, and varying the values does not change the qualitative conclusions. We consider randomly realized configurations with TLFs being $>1.5l_{QD}$ away from the centers of the QDs, which results in a relatively weak perturbation. The transfer Green's function can be treated approximately in a linear response manner.

We first model the transfer function term from the charge noise to a precession frequency. The electric field results in a displacement of the charge centroid of the confined electron. In the presence of a magnetic field gradient, it results in a fluctuation of the magnetic field. The in-plane displacement can be computed from the in-plane force [23],

$$\delta \vec{r}_{ik} = \delta x_{ik} \hat{x} + \delta y_{ik} \hat{y} = \frac{\vec{F}_{ik}}{m^* \omega^2}.$$
 (6)

In a device set up with the x-gradient of the magnetic field at the ith qubit dominates, $\frac{\partial B_i}{\partial x} >> \frac{\partial B_i}{\partial y}$ [14], the magnetic field variation due to position variation caused by the kth TLF charge is,

$$\delta B_{ik} \approx \frac{\partial B_i}{\partial x} \delta x_{ik} \tag{7}$$

In this study, we use a magnetic field gradient value of $\frac{\partial B_i}{\partial x} = 0.1 \mathrm{mT/nm}$, in the order of typical experimental value [6]. The charge noise of interest is low-frequency compared to the electrostatic response time. The Green's transfer function is treated as frequency-independent. Its element between fluctuation of the ith qubit precession frequency $\delta \nu_i$ and kth TLF is determined by

$$G_{ik} = \frac{g_i \mu_B}{h} \delta B_{ik},\tag{8}$$

where g_i is the g-factor and μ_B is the Bohr magneton, and δB_{ik} is computed with Eq. (7).

After obtaining the transfer function for single qubit terms, we derive the transfer function term from the charge noise to the exchange coupling between neighboring qubits. The exchange part of the effective Hamiltonian between a neighboring pair of qubits (i, j) is $H_{ex} = J_{ij} \left(\mathbf{S}_i \cdot \mathbf{S}_j - \frac{1}{4} \right)$ [28], [29], where $\mathbf{S}_{i \ or \ j}$ is the spin operator, and the exchange interaction J_{ij} can be expressed as,

$$J_{ij} = \frac{2t_{c,ij}^2}{U_{Hi} - \Delta_{ij}} + \frac{2t_{c,ij}^2}{U_{Hj} + \Delta_{ij}} = \frac{2t_{c,ij}^2 \left(U_{Hi} + U_{Hj} \right)}{\left(U_{Hi} - \Delta_{ij} \right) \left(U_{Hj} + \Delta_{ij} \right)}$$

where $t_{c,ij}$ is the tunnel coupling, Δ_{ij} is the detuning, and the Hubbard on-site double-occupancy potential values are assumed to be equal $U_{Hi} = U_{Hj} = U_H$, which is insensitive

to the TLF charge. For a two-qubit quantum gate as shown in Fig. 1, there is only one exchange term between left and right QDs. The expression simplifies to

$$J_{ij} = \frac{4t_{c,ij}^2 U_H}{U_H^2 - \Delta_{ij}^2} \tag{10}$$

The electric field by the TLF perturbs both the tunnel coupling $t_{c,ij}$ and detuning Δ [30]. Biasing the DQD structure at the sweet spot in which $\Delta \ll U_H$ helps to reduce the impact of charge noise [31]. At this bias condition, the tunnel noise dominates [30]

$$\delta J_{ij} \approx \frac{2J_{ij}\delta t_{c,ij}}{t_{c,ij}} \tag{11}$$

The tunnel coupling $t_{c,ij}$ depends on the tunnel barrier height and thickness between neighboring qubits. The tunnel coupling between two neighboring qubits can be numerically computed with a Schrödinger-Poisson solver [32]. The numerically computed tunnel coupling value can be well described by an analytical expression in the form of the WKB approximation, which is expressed as [30], [32],

$$t_{c,ij} = t_{c0} exp \left(-\frac{\sqrt{2qm^* E_{b,ij}}}{\hbar} L_{s,ij} \right), \tag{12}$$

where $E_{b,ij}$ is the barrier height and $L_{s,ij}$ is the spacing between the double quantum dots, and t_{c0} is a tunnel coupling parameter independent of $E_{b,ij}$ and $L_{s,ij}$. The tunnel coupling parameter can be obtained by fitting Eq. (12) to the numerical simulation results of the tunnel coupling values at different QD spacings and barrier heights [32]. The extracted pre-coefficient t_{c0} depends on the semiconductor material and carrier type. For silicon electrons, its value is in the order of $t_{c0} \approx 10 meV$ [32]. The perturbations of the barrier height and thickness due to a TLF with an in-plane distance of > 10 nm away from the quantum dot centers are orders of magnitude smaller than the barrier height and thickness themselves, and the fluctuation of the tunnel coupling can be approximately expressed as,

$$\frac{\delta t_{c,ij}}{t_{c,ij}} \approx \left(-\frac{\sqrt{2qm^*E_{b,ij}}}{\hbar} L_{s,ij}\right) \left(\frac{\delta L_{s,ij}}{L_{s,ij}} + \frac{\delta E_{b,ij}}{2E_{b,ij}}\right) \tag{13}$$

The kthe TLF perturbs the interdot spacing and the tunnel spacing,

$$\delta L_{s,ij} = \delta x_{ik} - \delta x_{jk} = \frac{F_{x,ik}}{m\omega_i^2} - \frac{F_{x,jk}}{m\omega_i^2}$$
 (14)

where F_x is the x-component of the electrostatic force. The change of the barrier height due to the TLF charge is computed by averaging over the tunneling path,

$$\delta E_{b,ij} = \frac{\int_{x_i}^{x_j} V_{TLF}(x, y = 0) \, dx}{x_j - x_i}$$
 (15)

The matrix element of Green's transfer function between an exchange interaction term δJ_{ij} and the kth TLF is obtained by substituting Eq. (13) to Eq. (11)

$$G_{J_{ij},k} = 2J_{ij} \left(-\frac{\sqrt{2qm^* E_{b,ij}}}{\hbar} L_{s,ij} \right) \left(\frac{\delta L_{s,ij}}{L_{s,ij}} + \frac{\delta E_{b,ij}}{2E_b, ij} \right),$$
(16)

where $\delta L_{s,ij}$ is computed by Eq. (14) and $\delta E_{b,ij}$ is computed from Eq. (15).

III. RESULTS

As an example, the simulation framework above is applied to a two-qubit quantum gate device as shown in Fig. 1. The spacing between the two QD centers is L_S =40nm. Both the Si layer and SiGe layer are assumed to have a thickness of 10nm. We examine the noise auto-correlation and cross-correlation of the precession rates of the left and right qubits, ν_L and ν_R respectively, and the exchange interaction between the qubits, J. For the device, the vector of physical quantities of interest is $P = [\nu_L, \nu_R, J]$. The auto-PSD values are derived from the diagonal elements of the matrix S(f) in Eq. (1), labeled as S_L , S_R , and S_J corresponding to ν_L , ν_R , and J, respectively. Cross-correlation values are computed using Eq. (2) and are represented by the symbol C with appropriate subscripts.

The charge noise dominates in an isotopically purified Si^{28} . The nuclear magnetic mechanism is weak, which can lead to a corresponding dephasing time $T_2^{nu}>100\mu S$. Spin-orbit-coupling is also weak in silicon [2]. We first focus on the case with charge noise only. The distribution of TLFs is randomly generated. To explore the statistical average values. We stochastically generate the TLF configurations with a density of $N_T=4\times10^{11}/cm^2$ uniformly distributed in the capping SiGe layer.

To explore the statistical average over random realizations of TLF configurations, we realize N_{config} =8000 configurations of the TLFs stochastically and compute the expectation values of noise correlation spectrums by averaging over these configurations. Fig. 2a shows that the expected auto-PSDs of the precession frequencies of two qubits are essentially equal, and show a 1/f noise scaling behavior. Each individual TLF produces a Lorentzian power spectrum. In calculating the expectation over a larger number of random TLF realizations, summing and averaging over Lorentzian with different corner frequency values leads to a 1/f scaling behavior of the expectation value. Similarly, the expectation value of the auto-PSD of the exchange interaction shows a clear 1/f scaling behavior. Fig. 2b shows the cross-PSD of the precession frequencies of two QDs. Both the expectation values of the amplitude and phase are nearly independent of the frequency. The expected amplitude is $\bar{A} \approx 0.5$ and the expected phase is $\phi \approx \pi/2$. For each configuration at a given frequency, the cross-correlation can be either in-phase ($\phi = 0$) or out-ofphase $\phi = \pi$. The phase expectation value is the statistical average of in-phase and out-of-phase correlations in random TLF realization. The results indicate a strong cross-correlation of the precession frequency noise between neighboring qubits.

Next, we examine the noise correlation of one randomly realized configuration of TLFs in the silicon spin qubit device.

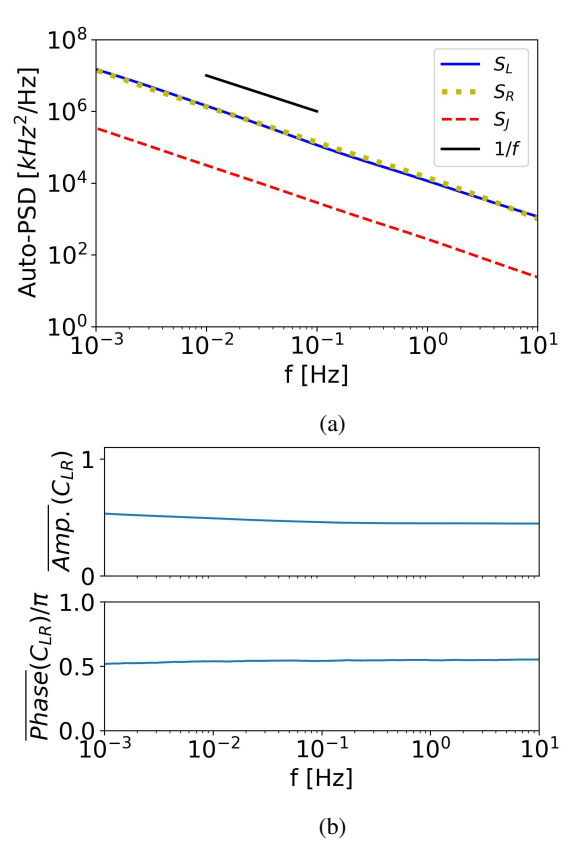


Fig. 2: (a) The expectation value of the auto-PSDs of the precession frequencies, S_L (blue solid) and S_R (green dotted), and the exchange interaction S_J (red dashed), over random TLF distributions. A reference line of 1/f scaling is also shown (black). (b) The amplitude (top) and phase (bottom) of the expectation value of the cross-PSD, C_{LR} between the precession frequencies of two qubits. The expectation values are computed by using 8000 random realizations of the TLF distributions.

Fig. 3a shows the noise auto-PSD S_L of the precession frequency of the left qubit. Fig. 3b shows the top view of the TLF distribution and the electron probability density of two spin qubits. We also simulated the PSD due to an individual TLF only as shown by the dotted line for TLF 1 and the dashdot line for TLF 2 in Fig. 3a. The results show that the total PSD can be well described by the sum of the PSDs from these two contributors. Each TLF charge results in a Lorentzian PSD, which is nearly constant at a frequency lower than its corner frequency and scales as $1/f^2$ at high frequencies. The sum of the contributions by TLFs 1 and 2 results in a 1/fscaling of their values at the corner frequencies, as shown by the slope of the black dashed line in Fig. 3a. These two charges have a dominant contribution because they have corner frequencies in the frequency range of interest and they are close to the left QD as shown in Fig. 3b.

The investigation of noise correlation between neighboring qubits has been conducted experimentally [14]. The study reveals pronounced cross-correlation and a phase-flipping char-

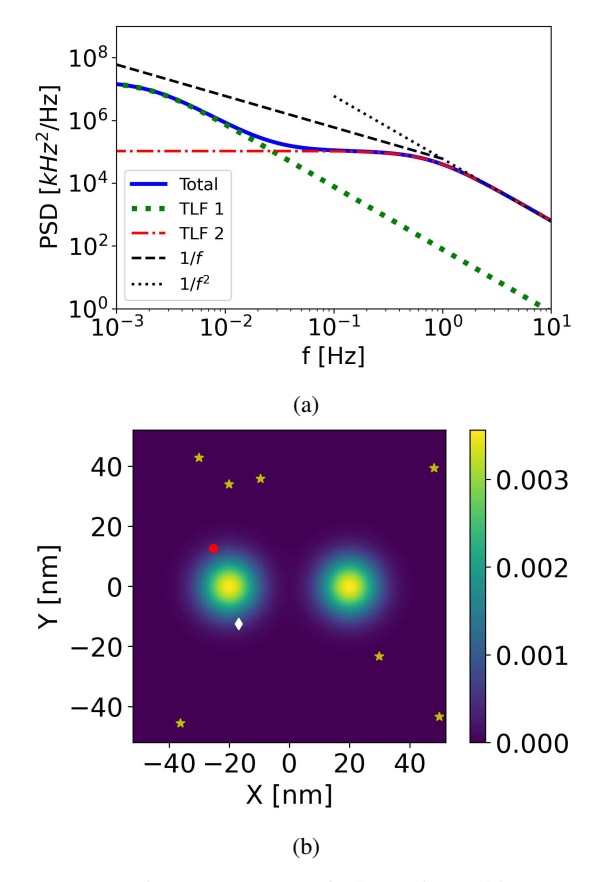


Fig. 3: (a) Noise auto-PSD of the spin qubit precession frequency at the left QD S_L (Solid) for the TLF configuration in (b). The auto-PSDs due to charge in TLF 1 and TLF 2 as denoted in (b) are shown by the green dotted and red dash-dot lines, respectively. 1/f and $1/f^2$ scaling lines are also shown. (b) A randomly realized TLF configuration and the pseudo-color plot of the electron probability density. All TLF charges are shown by scattered symbols. Two TLF charges with dominant contributions to the noise correlations in the frequency range of interest are denoted as the white diamond (TLF 1) and the red circle (TLF 2), and the rest TLF charges are denoted as yellow stars. The modeled device structure is shown in Fig. 1. The QD spacing is L_S =40nm with the QD centers located at (\pm 20nm,0).

acteristic, transitioning from out-of-phase to in-phase within the explored frequency range. We next investigate the cross-correlation of noise between two qubits. The cross-PSD C_{LR} between ν_L and ν_R is shown in Fig. 4. The results show a qualitative feature drastically different from the expectation value as shown in Fig. 2b, which highlights the importance of a small number of random discrete TLF charges. The cross-PSD flips from out-phase with $\phi=\pi$ at lower frequencies to in-phase with $\phi=0$ at higher frequencies. The amplitude indicates strong cross-correlation, with the peak value approaching the maximum correlation value of 1.

The reason for the out-phase to in-phase transition is explained as follows. As discussed before, TLFs 1 and 2 as shown in Fig. 3b have dominant contributions. TLF 1 is

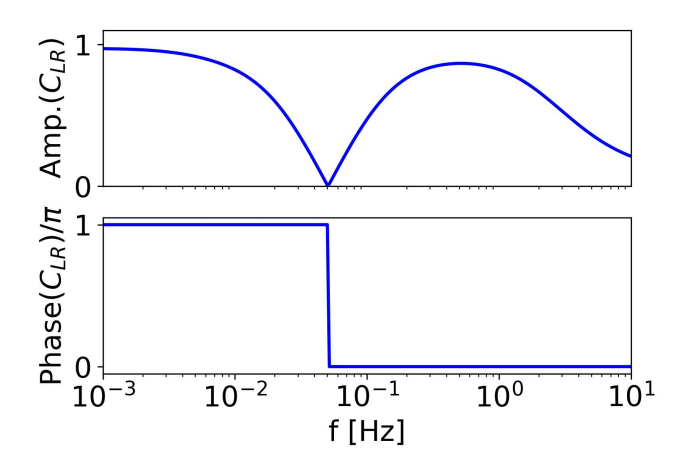


Fig. 4: The amplitude (top) and phase(bottom) of the cross-PSD C_{LR} between the precession frequencies of two qubits. The modeled device structure is the same as Fig. 3.

located at a x position between the charge centroids of the left and right qubit charge. Charge of the TLF 1 results in electrostatic forces that move two qubits charges along the opposite x directions. In contrast, TLF 2 is located to the left of both QDs. Its charge results in electrostatic forces that move both qubit charges along the same x direction. In the presence of a magnetic field gradient along x direction, the cross-PSD due to TLF 1 is out-phase, and that due to TLF 2 is in-phase. As shown in Fig. 3a, TLF 1 has a lower corner frequency and is more dominant at lower frequencies, and TLF 2 is more dominant at higher frequencies. As the frequency increases, the cross-PSD encounters a phase flip. Although a quantitative comparison between theory and experiment is hindered by random spatial and temporal distribution of TLFs, the simulation results share the same feature of phaseflipping as observed in experiments [6]. The results indicate the importance of discrete TLFs on noise correlation spectrums in a silicon spin qubit system.

IV. CONCLUSION

Noise presents a significant obstacle in improving fidelity and scalability for semiconductor-based quantum computing. In this work, we develop Green's transfer function method to analyze noise power spectral density and correlations in a silicon spin qubit system. This method involves mapping the behavior of charge noise sources of TLFs to the correlated noise PSDs of precession frequencies and exchange interactions in silicon spin qubit devices. Our findings highlight pronounced cross-correlations of noise. The impact of a small number of TLFs is notably significant due to the small scale of these devices, emphasizing the importance of their discrete and stochastic nature in silicon spin qubit operations. Simulations show that the noise correlation PSDs for a given TLF configuration can vary significantly from what statistical averages suggest. Additionally, our results shed light on the phase-flipping behavior observed in the cross-PSD noise of silicon spin qubit devices. The developed modeling technique is valuable for assessing and understanding noise correlations in semiconductor spin qubit systems, paving the way for future strategies to reduce the effects of correlated quantum noise.

REFERENCES

- A. A. Clerk, M. H. Devoret, S. M. Girvin, F. Marquardt, and R. J. Schoelkopf, "Introduction to quantum noise, measurement, and amplification," *Reviews of Modern Physics*, vol. 82, no. 2, p. 1155, 2010.
- [2] G. Burkard, T. D. Ladd, A. Pan, J. M. Nichol, and J. R. Petta, "Semiconductor spin qubits," *Reviews of Modern Physics*, vol. 95, no. 2, p. 025003, 2023.
- [3] M. A. Eriksson, M. Friesen, S. N. Coppersmith, R. Joynt, L. J. Klein, K. Slinker, C. Tahan, P. Mooney, J. Chu, and S. Koester, "Spin-based quantum dot quantum computing in silicon," *Quantum Information Processing*, vol. 3, pp. 133–146, 2004.
- [4] L. M. Vandersypen and M. A. Eriksson, "Quantum computing with semiconductor spins," *Physics Today*, vol. 72, no. 8, pp. 38–45, 2019.
- [5] E. J. Connors, J. Nelson, H. Qiao, L. F. Edge, and J. M. Nichol, "Low-frequency charge noise in si/sige quantum dots," *Physical Review B*, vol. 100, no. 16, p. 165305, 2019.
- [6] J. Yoneda, K. Takeda, T. Otsuka, T. Nakajima, M. R. Delbecq, G. Allison, T. Honda, T. Kodera, S. Oda, Y. Hoshi *et al.*, "A quantum-dot spin qubit with coherence limited by charge noise and fidelity higher than 99.9%," *Nature Nanotechnology*, vol. 13, no. 2, pp. 102–106, 2018.
- [7] M. Veldhorst, C. Yang, J. Hwang, W. Huang, J. Dehollain, J. Muhonen, S. Simmons, A. Laucht, F. Hudson, K. M. Itoh *et al.*, "A two-qubit logic gate in silicon," *Nature*, vol. 526, no. 7573, pp. 410–414, 2015.
- [8] M. T. Madzik, S. Asaad, A. Youssry, B. Joecker, K. M. Rudinger, E. Nielsen, K. C. Young, T. J. Proctor, A. D. Baczewski, A. Laucht et al., "Precision tomography of a three-qubit donor quantum processor in silicon," *Nature*, vol. 601, no. 7893, pp. 348–353, 2022.
- [9] S. G. Philips, M. T. Madzik, S. V. Amitonov, S. L. de Snoo, M. Russ, N. Kalhor, C. Volk, W. I. Lawrie, D. Brousse, L. Tryputen *et al.*, "Universal control of a six-qubit quantum processor in silicon," *Nature*, vol. 609, no. 7929, pp. 919–924, 2022.
- [10] X. Xue, M. Russ, N. Samkharadze, B. Undseth, A. Sammak, G. Scappucci, and L. M. Vandersypen, "Quantum logic with spin qubits crossing the surface code threshold," *Nature*, vol. 601, no. 7893, pp. 343–347, 2022.
- [11] L. Kranz, S. K. Gorman, B. Thorgrimsson, Y. He, D. Keith, J. G. Keizer, and M. Y. Simmons, "Exploiting a single-crystal environment to minimize the charge noise on qubits in silicon," *Advanced Materials*, vol. 32, no. 40, p. 2003361, 2020.
- [12] B. Paquelet Wuetz, D. Degli Esposti, A.-M. J. Zwerver, S. V. Amitonov, M. Botifoll, J. Arbiol, A. Sammak, L. M. Vandersypen, M. Russ, and G. Scappucci, "Reducing charge noise in quantum dots by using thin silicon quantum wells," *Nature Communications*, vol. 14, no. 1, p. 1385, 2023.
- [13] F. Ye, A. Ellaboudy, D. Albrecht, R. Vudatha, N. T. Jacobson, and J. M. Nichol, "Characterization of individual charge fluctuators in si/sige quantum dots," arXiv preprint arXiv:2401.14541, 2024.
- [14] J. Yoneda, J. Rojas-Arias, P. Stano, K. Takeda, A. Noiri, T. Nakajima, D. Loss, and S. Tarucha, "Noise-correlation spectrum for a pair of spin qubits in silicon," *Nature Physics*, vol. 19, no. 12, pp. 1793–1798, 2023.
- [15] A. Saraiva, W. H. Lim, C. H. Yang, C. C. Escott, A. Laucht, and A. S. Dzurak, "Materials for silicon quantum dots and their impact on electron spin qubits," *Advanced Functional Materials*, vol. 32, no. 3, p. 2105488, 2022.
- [16] F.-C. Hou, G. Bosman, and M. E. Law, "Simulation of oxide trapping noise in submicron n-channel mosfets," *IEEE Transactions on Electron Devices*, vol. 50, no. 3, pp. 846–852, 2003.
- [17] C. Müller, J. H. Cole, and J. Lisenfeld, "Towards understanding two-level-systems in amorphous solids: insights from quantum circuits," *Reports on Progress in Physics*, vol. 82, no. 12, p. 124501, 2019.
- [18] M. Chen, J. C. Owens, H. Putterman, M. Schäfer, and O. Painter, "Phonon engineering of atomic-scale defects in superconducting quantum circuits," arXiv preprint arXiv:2310.03929, 2023.
- [19] A. Ayachi, W. B. Chouikha, S. Jaziri, and R. Bennaceur, "Telegraph noise effects on two charge qubits in double quantum dots," *Physical Review A*, vol. 89, no. 1, p. 012330, 2014.
- [20] E. Paladino, Y. Galperin, G. Falci, and B. Altshuler, "1/f noise: Implications for solid-state quantum information," *Reviews of Modern Physics*, vol. 86, no. 2, p. 361, 2014.

- [21] L. Petit, J. Boter, H. Eenink, G. Droulers, M. Tagliaferri, R. Li, D. Franke, K. Singh, J. Clarke, R. Schouten *et al.*, "Spin lifetime and charge noise in hot silicon quantum dot qubits," *Physical Review Letters*, vol. 121, no. 7, p. 076801, 2018.
- [22] S. Ahn, S. D. Sarma, and J. Kestner, "Microscopic bath effects on noise spectra in semiconductor quantum dot qubits," *Physical Review B*, vol. 103, no. 4, p. L041304, 2021.
- [23] M. M. E. K. Shehata, G. Simion, R. Li, F. A. Mohiyaddin, D. Wan, M. Mongillo, B. Govoreanu, I. Radu, K. De Greve, and P. Van Dorpe, "Modeling semiconductor spin qubits and their charge noise environment for quantum gate fidelity estimation," *Physical Review B*, vol. 108, no. 4, p. 045305, 2023.
- [24] P. Dutta and P. Horn, "Low-frequency fluctuations in solids: 1 f noise," *Reviews of Modern physics*, vol. 53, no. 3, p. 497, 1981.
- [25] J. H. Davies, The physics of low-dimensional semiconductors: an introduction. Cambridge university press, 1998.
- [26] D. Culcer, X. Hu, and S. Das Sarma, "Dephasing of si spin qubits due to charge noise," *Applied Physics Letters*, vol. 95, no. 7, 2009.
- [27] S. D. Sarma, X. Wang, and S. Yang, "Hubbard model description of silicon spin qubits: Charge stability diagram and tunnel coupling in si double quantum dots," *Physical Review B*, vol. 83, no. 23, p. 235314, 2011.
- [28] T. Meunier, V. E. Calado, and L. M. Vandersypen, "Efficient controlledphase gate for single-spin qubits in quantum dots," *Physical Review B*, vol. 83, no. 12, p. 121403, 2011.
- [29] D. M. Zajac, A. J. Sigillito, M. Russ, F. Borjans, J. M. Taylor, G. Burkard, and J. R. Petta, "Resonantly driven cnot gate for electron spins," *Science*, vol. 359, no. 6374, pp. 439–442, 2018.
- [30] P. Huang, N. M. Zimmerman, and G. W. Bryant, "Spin decoherence in a two-qubit cphase gate: the critical role of tunneling noise," npj Quantum Information, vol. 4, no. 1, p. 62, 2018.
- [31] F. Martins, F. K. Malinowski, P. D. Nissen, E. Barnes, S. Fallahi, G. C. Gardner, M. J. Manfra, C. M. Marcus, and F. Kuemmeth, "Noise suppression using symmetric exchange gates in spin qubits," *Physical Review Letters*, vol. 116, no. 11, p. 116801, 2016.
- [32] T. Wu and J. Guo, "A multiscale simulation approach for germanium-hole-based quantum processor," *IEEE Transactions on Computer-Aided Design of Integrated Circuits and Systems*, vol. 42, no. 1, pp. 257–265, 2022.